A selective chemosensor for fluoride ion and its interaction with Calf Thymus DNA

Soumen Ghosh, Abdulla Al Masum, Aniruddha Ganguly, Md. Maidul Islam, Md. Akhtarul Alam, Nikhil Guchhait

PII: S1386-1425(17)30063-X
DOI: doi: 10.1016/j.saa.2017.01.044
Reference: SAA 14897

To appear in: *Spectrochimica Acta Part A: Molecular and Biomolecular Spectroscopy*

Received date: 26 July 2016
Revised date: 21 January 2017
Accepted date: 23 January 2017

Please cite this article as: Soumen Ghosh, Abdulla Al Masum, Aniruddha Ganguly, Md. Maidul Islam, Md. Akhtarul Alam, Nikhil Guchhait , A selective chemosensor for fluoride ion and its interaction with Calf Thymus DNA. The address for the corresponding author was captured as affiliation for all authors. Please check if appropriate. Saa(2017), doi: 10.1016/j.saa.2017.01.044

A selective chemosensor for fluoride ion and its interaction with Calf Thymus DNA

Soumen Ghosh[a], Abdulla Al Masum[b], Aniruddha Ganguly[a], Md. Maidul Islam[b], Md. Akhtarul Alam[b]*and Nikhil Guchhait[a]*

[a]Department of Chemistry

University of Calcutta

92, A.P.C. Road, Kolkata 700 009, India

Telephone 91-33-23508386

Fax: 91-33-23519755

[b]Department of Chemistry

Aliah University

IIA/27, New Town, Kolkata-700 156, West Bengal, India

*Corresponding author, E-mail: alam_iitg@yahoo.com (M.A. A.);

and

nguchhait@yahoo.com (N.G.)

Abstract

The amido-Schiff base **1** (*N^1, N^3-bis (2-nitrobenzylidene)benzene-1,3-dicabohydrazide*) containing a –CONH- group and –CH=N- linkage has been synthesized by the condensation between Isophthalic acid dihydrazide and *o*-nitrobenzaldehyde. This molecule can act as a fluoride ion sensor with high selectivity and sensitivity. Presence of nitro group in the phenyl ring may be responsible for the detection of fluoride ion visually with a dramatic color change from colorless to deep red in aqueous dimethylsulphoxide solution. This Schiff base can be used as test kit for sensing of fluoride ion in the solid state. Compound **1** can detect fluoride also in commercially available toothpaste. As the compound has adequate solubility in DMSO-water mixture (7 : 93, v/v) and having some hydrogen bond donor and acceptor centers, we have investigated its nature of binding with Calf Thymus-DNA (CT-DNA) using theoretical molecular modelling and other experimental methods like UV−Vis spectroscopy, circular dichroic and thermal melting studies. Thermodynamic parameters have been obtained using the well known vant Hoff's equation. From both theoretical and experimental findings it has been observed that it can interact effectively with CT-DNA with binding energy -7.55kcal/mol to -7.50 kcal/mol.

Key Words: Colorimetric sensing, F^- sensor, Schiff base, Hydrogen bonding, DNA interaction

1. Introduction

In recent time, the design and synthesis of artificial molecules which are capable to interact with biologically important molecules and ions are the basis of medicinal or clinical research activities to study the biophysical and biochemical processes. One of them is the detection of fluoride ion because of its unique properties compared to its congeners and its significant role for biological and industrial applications [1-2]. For example, fluoride salts are commonly used in some biological processes to inhibit the activity of phosphatases in serine/threonine phosphatases enzymes active sites [3-5]. Sometimes, it is used as an important constituent in most of the drug molecules for the treatment of anesthetics, hypnotics' psychiatric drugs and cockroach poisons [6-7]. Moreover, fluoride is an essential element in human diet due to its significant role in bone and teeth mineralization [8-9]. But excessive fluoride intake may cause bone disorders, thyroid activity, collagen breakdown depression and immune system disruption [10-11]. This dual functionality of fluoride ion has acquired interest to the chemists. For this purpose a number of procedures have been reported for the detection of fluoride [12-16]. Among them the use of electrode is very familiar. However, this procedure is too much laborious, time consuming and costly [16-19]. On the other hand, fluorescence based sensors require some instrumental assistance and they are less useful in real-time application [20]. In contrast, colorimetric receptors received much attraction to the analyst because of simplicity, sensitivity, selectivity and real-time 'naked eye' detection without help of any instrument.

The visual detection of fluoride can be achieved by designing a host molecule which can change its color during the detection process and colorimetric sensors are the

best for this purpose. Generally a colorimetric sensor contains a binding site (H-bond donors) to interact with anions and a signaling unit (e.g. $–NO_2$ group) to show the color changes during the interaction of the sensor and the anions. Based on this concept, lots of sensors have been reported. However very few of them are able to detect fluoride selectively [21-23]. Furthurmore most of them are unable to detect fluoride in solid state which is no doubt a restriction of their application.

Another interesting field is the study of the interaction between synthetic organic small molecules/drugs/drug templates with DNA, because it provides the opportunity to develop a new efficient therapeutic agent to control gene expression [24-25]. The interaction of small molecules with DNA involves mainly three modes- (i) intercalation of the molecule within the base pairs of nucleic acid to distort the DNA backbone (ii) groove binding in the deep major groove or the shallow minor groove of the DNA helix by some non-bonding interactions (like hydrogen bonding or van der Waals interaction) and (iii) electrostatic binding between the negatively charged DNA phosphate backbone and cationic or positive end of the molecules [26-27]. These studies can provide significant information about various important biological processes and to design and develop of new and more efficient therapeutic agents targeted to DNA.

Considering the above facts we have synthesized and characterized a amido-Schiff base **1**, as molecular sensor for fluoride and studied its interaction with DNA. Here, the compound **1** detects fluoride ion selectively in semi-aqueous medium as well as in solid state by a naked-eye color change from colorless to deep red. Interestingly, it has been found that the position of $–NO_2$ group in the compund has an effect on the sensitivity as well as on the color change. Furthuemore, compound 1 has been found to interact

effectively with calf-thymus DNA established by both experimental and theoritical results.

2. Experimental

2.1. Instrumentation

Electronic absorption spectra have been recorded by a Hitachi UV-Vis (Model U–3501) spectrophotometer. IR spectra (KBr pellet, 4000–400 cm^{-1}) have been recorded on a Parkin Elmer modal 883 infrared spectrophotometer. ^{1}H NMR spectra have been recorded on a Bruker, Avance 300 spectrometer, where chemical shifts (δ in ppm) have been determined with respect to tetramethylsilane (TMS) as internal standards. The intrinsic circular dichroism (CD) spectra have been recorded on a JASCO J-815 spectropolarimeter using a cylindrical cuvette of 0.1 cm path length at 25 ^{0}C.

2.2. Reagents

All reagents and solvents required for synthesis have been used as received from commercial sources without further purification. All anions in the form of tetrabutylammonium salts have been purchased from Sigma-Aldrich Chemical Company. All solvents used for the spectroscopic studies are spectroscopic grade. Calf-thymus DNA from Sigma-Aldrich, USA, has been used as received. Disodium hydrogen phosphate and citric acid have been purchased from SRL, India, and citrate-phosphate buffer of pH 7.4 was prepared in triply distilled deionized water from a Milli-Q water purification system (Millipore).

2.3. Syntheses

The Isophthalic acid dihydrazide (**A**) has been synthesized accroding to the literature procedure [28].

2.3.1. Compound 1: Sythesis of *N^1, N^3-bis (2-nitrobenzylidene)benzene-1,3-dicabohydrazide*

Compound **A** (1 mmol, 0.200 g) has been reacted with 2-nitrobenzaldehyde (2.3 mmol, 0.350 g) in methanol at room temperature for 30 minutes and a very light yellow solid has been obtained. The product thus obtained has been filtered and then dried under vacuum (yield: 0.330 g, 70%). ^{1}H NMR in d_6-DMSO, 300MHz, δ (ppm): 12.37 (s, 2H, –CONH–), 8.88 (s, 2H, –CH=N–), 8.49 (s, 1H), 8.15-8.06 (m, 6H), 7.82 (t, J=7.5 Hz, 2H), 7.7-7.65 (m, 3H). ^{13}C NMR (75.5 MHz, d_6-DMSO, 20 ºC) δ (ppm): 124.89, 128.28, 128.85, 131.03, 131.42, 133.54, 133.99, 143.76, 148.52, 163.03. Anal. calcd for C22H16N6O6: C, 57.39; H, 3.50; N, 18.25. Found: C, 57.32; H, 3.58; N, 18.20. IR (KBr): 3235, 3190, 3049, 1677, 1644, 1541, 1517, 1361, 1339, 1282, 1262, 1160, 1126 cm^{-1}.

3. Results and discussion

The compound **1** has been synthesized following two steps (Scheme I). In the first step isophthalic acid dihydrazide has been prepared from diethyl isophthalate, then condensation was done with *o*-nitro benzaldehyde, Compound **1** has been characterized by ^{1}H, ^{13}C NMR and IR spectroscopic methods. The FT-IR spectrum provides the information about the presence of two functional groups (amido (–CONH–) and imino (–CH=N–) group) by the absorption peaks in the range of 1677 to 1665 and 1660-1644 cm-

$^{-1}$ respectively [29]. In the ^{1}H-NMR spectra, two characteristic peaks at 12.37 ppm and 8.88 ppm have been found which also support the presence of (–CONH–) and imino (–CH=N–) groups in compound **1** [30].

3.1. Visual sensing of anions

The colorimetric sensing ability of compound **1** (10^{-4} M) has been investigated by naked eye in aqueous dimethyl sulphoxide solvent (DMSO:H_2O =7:3, v/v). When F^- ion is added to the solution of **1**, an intense red coloration occurs, which can be visualized by naked eye (Fig. 1). Now to rationalize the reason behind the color change of compound **1**, we have synthesized two copounds (**2** and **3**, Scheme 1). Compound **2** contains the nitro group in the meta position of the aldehyde ring and compound **3** does not contain nitro group. On treatment of F^- with the aqueous DMSO solution of **2** and **3** (1.0×10^{-4} M) , **2** shows a color change from colorless to light yellow (Fig. S9), but **3** does not show any color change (Fig. S10). So, the colour change of the compound are most probably due to hydrogen bonding interaction between the amide groups and fluoride ion. The formation of these hydrogen bonds affects the electronic properties of the chromophore, leading to a subsequent intramolecular charge-transfer from electron rich fluoride-bound amide to the electron deficient nitrobenzene group in compounds **1** and **2** [31-32].

Under similar experimental condition, other anions, such as CH_3COO^-, $H_2PO_4^-$, Cl^-, Br^-, HSO_3^- and CN^- do not exhibit any visual color change which attributes either very negligible or no interaction of these anions with the compounds. Based on the above obervations, it can be said that compound **1** can detect fluoride ion selectively.

3.2. UV–Vis spectroscopic titration

The colorimetric sensing ability of compound **1** (10^{-6} M) with anions has also been monitored by UV-Visible spectroscopy in aqueous dimethyl sulphoxide solution. Compound **1** exhibits a strong absorption band at 300 nm and a hump at 335 nm (Fig. 2 and Fig. S11). With the addition of increasing amount of F^- ion to the aqueous dimethyl sulphoxide solution of **1** (10^{-6} M), the peak at 300 nm gradually decreases with the generation of a shoulder band slightly shifted to red with increasing intensity and a new broad absorption band appears at 456 nm with a clear isosbestic point at 345 nm. The presence of one isosbestic point indicates one type of interaction takes place between **1** and F^- which is obviously the formation of complex between **1** and the fluoride ion via H-bonding interaction. As a result the –N centre of the amide becomes electron rich resulting a intramolecular charge transfer from the electron rich amidic nitrogen to the electron deficient $–NO_2$ group and this is the reason for the appearance of the new band at at 456 nm. To cross check our assumption, i.e. the effect of nitro group on the color change of the compound **1** towards fluoride, we have studied the UV-Vis responses of compound **2** and **3** in presence of fluoride in aqueous DMSO solution. The UV-Vis spectra of compound **2** (10^{-6} M) also show an observable change during titration with F^- ion. Upon addition of F^- ion, the peak at 274 nm decreases its intensity, while a new band at 343 nm appears with an isosbestic point at 317 nm (Fig. S12). These spectral changes take place accompanied by visual color change from colorless to yellow color. As expected, the UV-Vis spectrum of compound **3** does not show any notable spectral changes with addition of increasing amount of F^- ion (Fig. S13). These spectral changes also gives the evidence for the formation of H-bonded complex between the two amide

protons of the compound and F^- ion followed by deprotonation of the protons which gets stabilized by resonance with the $–NO_2$ group [33-34]. The compound **1** containing the nitro group in ortho position shows red shifted band for fluoride complex than fluoride complex of **2** where the nitro group is in the meta position. This is because the nitro group in the ortho position makes the amide proton more acidic and at the same time it makes more stable fluoride complex by resonance stabilization (Scheme 2 and S1). Under the same experimental condition, on addition of other anions such as AcO^-, $H_2PO_4^-$, Cl^-, Br^-, I^- and HSO_3^- notable spectral or colour changes have not been observed with **1**, **2** and **3** indicating no interaction or complexation of these anions with the above the compounds (Fig. S8, S9a, S10).

As shown in Fig. 2 (inset), the Benesi–Hildebrand (B–H) plot of $1/[A\text{-}A_0]$ vs $1/[F^-]$ for the titration of **1** with F^- ion provides a stright line, indicating 1:1 complex formation with association constant (K) 1.3×10^3 M^{-1} [35-36]. The detection limit of sensor **1** towards F^- ion has been calculated using UV–Visible titration data (Fig. S14). Sensor **1** is found to have a detection limit of 1.2×10^{-6} M for F^- in semi aqueous solvent system [37].

3.3. ^{1}H NMR titration

To investigate the nature of binding of compound with fluoride ion, ^{1}H NMR titration experiments have been performed in d_6-DMSO. ^{1}H NMR spectra of **1** shows characteristic peak of amide proton (H_a) at δ 12.37 ppm (Fig. 3). During titration when 1 equiv. of TBAF has been added the –NH peak becomes broad due to the formation of H-bonded complex. On further addition of 2 equiv. of F ions the –NH peak of receptor **1**

disappears and the H_c proton of isophthalate undergoes an downfield shift. At 5 equivalent of F^- ions the H_c proton is further shifted to downfield direction, at the same time the signal at δ 8.88 corresponding to imine proton H_b is slowly upfielded owing to the formation of exocyclic double bond during detection process. The downfield shift of H_c proton of isophthalate may be explained in terms of hydrogen bonding interaction between the H_c proton and the fluoride ion (Scheme II) [38-39].

The above results of ^{1}H NMR titration and UV–Vis titration indicate that the binding mechanism of compound **1** with fluoride may be a two step process. Firstly, 1:1 adduct formation has been taken place between compound **1** and fluoride ion through hydrogen bonding interaction and then deprotonation of –NH- proton which increases electron density over the receptor. As a result charge separation is introduced in the receptor which triggers intramolecular charge transfer (ICT) between the electron deficient $–NO_2$ group and electron rich –N of amide to show the UV-Vis and colorimetric changes. In case of compound **1** the electron deficient $–NO_2$ group is in the ortho position of the phenyl ring which results better charge seperation between the donor moiety (electron rich –N of amide) and the acceptor moeity (electron deficient $–NO_2$ group) consequently the ICT process becomes energiticaly more favourable. As a result the compound **1** absorbs the longer wavelength resulting a color change from colorless to deep red (Scheme II and Scheme S2). In contrast, compound **2** has the $–NO_2$ group in the meta position. So extent of charge seperation will be less, therefore, the ICT process is comperatively less energiticaly favourable than **1**. That is why it absorbs comperatively shorter wave length than **1** showing a yellow coloration (Scheme S1). As compound **3** does not contain $–NO_2$ group in the phenyl ring, the amide protons are not sufficiently

acidic. So the extent of interaction of it with F^- will be less than the above two. If it interacts with F^- , due to absence of $–NO_2$ group there will be no effective charge seperation to favour ICT process. As a result no color change has been observed for it.

3.4. Practical Application

3.4.1. Visual color changes on test papers

By considering the above observations, we have tried to investigate practical applications of compound **1** as anion sensor. To explore this, we have prepared test kits by coating a test paper (Whatman-40) with aqueous DMSO solution of **1** (1×10^{-4} M) and then dried it in air for long time because it is hard to be dried in air. For the detection of anion, the aqueous solution of anions (1×10^{-4} M) have been added on the test paper and dried in hot air. Interestingly, only that spot which contains F^- ion shows a bright red color (Fig. 4) and no color changes was observed in other spots containing anions like AcO^-, Cl^-, Br^-, I^-, CN^-, HSO_3^- and $H_2PO_4^-$. This experiment supports that compounds **1** has the capability to detect F^- ion both in solution and solid state. It is noteworthy to mention that compound **2** can also detect fluoride ion in solid state exhibiting light yellow color on the test paper (Fig. S15).

3.4.2. Detection of fluoride in toothpaste by the compound 1

As we have mentioned above, compound **1** can quantitatively detect F^- in a very wide concentration range, we have checked the sensitivity of compound **1** towards fluoride ion in commercially available toothpaste. For this purpose we have prepared an aqueous DMSO solution of commercially available toothpaste as sample. With the

addition of the toothpaste solution to the aqueous DMSO solution of compound **1** (1×10^{-4} M) a deep yellow color generates which is comparable to the color of the receptor in presence of bare fluoride (Fig.S16, inset). The UV-Vis spectra of compound **1 (**1×10^{-5} M) in presence of toothpaste solution shows a broad band at 465 nm which is resemblance to the UV-Vis spectra of sensor **1** in presence of fluoride (Fig.S13). Thus the sensor **1** can detect F^- in commercially available toothpaste.

3.5. Theoretical structure

To know the most stable conformers of **1** and the reference compound **3** the ground state optimization has been carried out in vacuum using Gaussian 03 software with B3LYP hybride functional and 6-31++G(d,p) basis set at Density Functional Theory level [40]. The optimized global minimum structure of **1** shows that the two nitro-benzene moieties and the isophthalic moiety are not in the same plane and is twisted by an angle of 57.4^o (Fig. 5). The optimized structure of **1** also shows that each amide C=O is intramolecularly H-bonded with the N= C-H (distances H1….O1 and H2…O2 are 2.180Å and 2.180Å respectively, Table 1). Furthermore, the O atom of the NO_2 groups is also H-bonded with the N= C-H (distances H1….O3 and H2….O4 are 2.277Å and 2.277Å respectively, Table 1). Importantly the two amide N-H moieties are pointing upward with respect to the isophthalic moiety. The isophthalic moiety and the amide N-H are not in the same plane and are deviated by the tortional angle of 41.5^o. In case of compound 3 also the benzene moieties and the isophthalic moiety are not in the same plane (Fig. S17a). Unlike **1**, the immine hydrogens of **3** are pointed towards inside, perhaps the absence of $-NO_2$ group may be reason. That is why, there is no H-bonding

interactions between the carbonyl oxygens and the immine hydrogens. Now, the optimized structure **1**.F^- complex shows that fluoride ion can fit in-between the twisted structure of **1**, and thus can form 1:1 stable complex (Fig. S17b), where donor-acceptor distances are N-H3...F^- = 2.220 Å , N-H4...F^- = 1.692 Å and C-H5….F^- = 2.106 Å (Table 1). It is important to note that in **1**.F^- complex the O1-H1 and O2-H2 distances are changed compare to the bare compound **1** (Table 1). Furthermore, after complex formation the tortional angle between the isophthalic moiety and the anime N-H reduces to 22.59^o. Interestingly, the predicted stoichiometry from theoretical structural optimization corroborates with the outcome of UV-Vis titration experiment and B–H plot. On the other hand the optimized structure of 3.F^- complex shows that between two amidic hydrogen only H4 is in same plane with fluoride and there is a partial double bond character between N2 and the carbonyl carbon (Fig. S17c). That means only H4 forms effective H-bond with fluoride where the donor-acceptor distances are N-H3...F^- = 2.74 Å , N-H4...F^- = 2.12 Å and C-H5….F^- = 2.22 Å (Table S1). So it can be said that between compound **1** and **3**, compound **1** form strong complex with fluoride ion.

3.6. DNA binding Study

As compound **1** contains several H-bond donor acceptor units and most importantly it is soluble in water-DMSO solvent mixture (water : DMSO =93:7), we have investigated its interaction with calf-thymus DNA in Citrate Phosphate Bufffer containing 7% DMSO, [Na^+] 10 mM, pH 7.0).

3.6.1. Absorption spectral modification of 1 in presence of DNA

The absorption profile of compound **1** shows a strong absorption band at 300 nm and a hump at 335 nm. On addition of CT-DNA the absorption intensity decreases with slight red shift, indicating modification of the environment of compound **1** suggesting binding interaction of **1** and CT-DNA (Fig. 6). Non-cooperative Scatchard analysis (Fig.6, inset) has been used to determine binding constant and the number of excluded base pair during binding process [41]. Analysis of data shows that binding constant is 2.99×10^{5} M^{-1}, while the number of excluded base pair is 9.5. These data shows that compound **1** binds strongly to DNA .

3.6.2. Conformation investigation: circular dichroism spectroscopy

To further study the binding of compound **1** with CT-DNA, intrinsic CD spectra of CT-DNA has been measured at increasing volume of DMSO in water to examine its stability in water-DMSO mixture. The CD spectra reveal that the conformation of CT- DNA remains unchanged upto 50% DMSO (Fig. 7a). So we have studied the binding interaction of **1** with CT-DNA in 7% DMSO–water mixture which is very less than the permisiable level of stability of CT-DNA.

The CD spectra of CT-DNA in 7% DMSO exhibit a typical shape (Fig. 7b), revealing a minimum at ~ 247 nm and a maximum at ~ 276 nm corresponding to the right handed B-form. On addition of compound **1**, it has been found that molar ellipticity of positive band increases gradually. Two very weak isoelliptic points have also been observed at 292 and 262 nm which indicate strong binding of ligand to CT-DNA helix and change in conformation of CT-DNA due to binding with **1** (Fig. 7b) [42].

3.6.3. Thermodynamic parameters and nature of the acting forces

There are different types of binding interaction between small molecules and DNA such as hydrogen bond, van der Walls force, electrostatic and hydrophobic interaction. Since the sign and magnitude of the thermodynamic parameters (ΔH, ΔS, ΔG) can account for the main driving forces for these interactions, we have estimated these parameters from the plot of ln K_b vs 1/T (Fig. 8) according to the van't Hoff Eq. (Table S2). Ross and Subramanian have explained the thermodynamic law to evaluate the primary mode of binding forces between small molecules and biological molecules: (1) ΔH > 0 and ΔS > 0 are associated with hydrophobic interaction; (2) electrostatic force are more dominant when ΔH= 0 and ΔS > 0; (3) ΔH < 0 and ΔS < 0 are frequently taken for hydrogen bond and van der Waals force [43]. From the fitted data it has been observed that the enthalpy of binding (ΔH) is -1.3 kcal where as the entropy change (ΔS) during the binding is 20.8 cal/mol/K (Fig. 8). These data clearly shows that the binding is favored by negative enthalpy and positive entropy change. This infers groove binding between the molecule and DNA through hydrogen bonding and van der Waals interaction. As seen in Table S1, the negative values of ΔG signify that the process of probe-DNA interaction is spontaneous in nature.

3.6.4. DNA Denaturation Temperature Studies.

DNA melting experiment provides characteristic melting temperature (T_m) at which DNA double helix strands separates as a result of breaking of all type of non-bonding interactions. Depending on the strength of interaction between the molecule and DNA melting temperature varies. Here, the change in absorbance at 260 nm for the DNA in the

absence and presence of compound **1** has been measured. The values of T_m of DNA and the **1**-DNA system have obtained from the transition midpoint of the melting curves based on f_{ss} versus temperature (T),

$$f_{ss} = (A - A_0)/(A_f - A_0)$$

where A_0 is the initial absorbance intensity, A is the absorbance intensity corresponding to its temperature, and A_f is the final absorbance intensity [44]. The melting curves of DNA in the absence and presence of **1** is shown in Figure 9. As seen in the figure, the T_m of DNA in the absence of **1** is 71^oC, whereas T_m of DNA in the presence of **1** is 72.02^oC. The melting data indicates that the DNA helix stabilizes moderately on binding with **1**.

3.6.3. Molecular docking studies

To study the binding of compound **1** with CT-DNA docking calculations using MOE program have been conducted using Alpha PMI as the placement methodology with four CT-DNA sequences (Table 2). The docked poses obtained thus have been further refined using force field method available in the MOE program. The calculation setup has been approached by placing the compound **1** in the minor groove of CT-DNA and the search space has set to the pocket. This enabled the MOE program to search the binding poses in the minor groove only. Once compound **1** has been placed, the docking run has been initiated with the input parameters described above.

Molecular docking of compound **1** clearly reveals that due to the curve shape of compound **1** it prefers to bind to the narrower and deeper shape of the minor groove of CT-DNA and binding further stabilizes through hydrogen bonding and van der Waals forces (Fig. S18). The free energy of binding is in the range of -9.53 to -7.16 kcal/mol

which collaborates with the experimental value (Table S2). From the docking picture and two dimensional binding studies it is observed that the N-H group and the carbonyl group played a significant role during binding process forming hydrogen bond with bases present in DNA (Fig.10a and Fig. S19).

The orientation of compound **1** in the minor groove is such that its nitro group ring is orthogonal to the rest of the molecule and is exposed to the outside of the minor groove and in contact with solvent environment. It is also observed that the molecule occupied 5 to 7 base pair during binding to CT-DNA (Fig.10) which was supported by Scatchard plot.

4. Conclusion

In summary, we have described that isophthalic acid dihydrazide derived Schiff bases **1** containing electron deficent $–NO_2$ group can selectively detect F^- ion by changing color, which could be visible by "naked-eye" without any spectroscopic instrumentation both in solution phase and in solid phase. Interestingly, compound **1** interacts effectively with CT-DNA. Docking study, CD spectral analysis and thermal denaturation study suggest that binding of compound **1** to DNA is mainly groove binding in nature. Thermodynamic parameters show that the binding of **1** to DNA is favored by both negative enthalpy and positive entropy changes. So the compound **1** can be used as a colorimetric fluoride sensor in both solid and solution phase as well as it can act as a good DNA intercalater.

Acknowledgment

SG & AG would like to acknowledge UGC for Fellowship. MAA thanks DST, Govt. of West Bengal, India (Project No. 376(Sanc.)/ST/P/S&T/9G-16/2013) for financial support.

References

[1] C. R. Cooper, N. Spencer, T. D. James, Chem. Commum. (1998) 1365-1366.

[2] C. B. Black, B. Andrioletti, A. C. Try, C. Ruiperez, J. L. Sessler, J. Am. Chem. Soc. 121 (1999) 10438-10439.

[3] C. Nakai, J. A. Thomas, J. Biol. Chem. 249 (1974) 6459-6467.

[4] W. Wang, H. S. Cho, R. Kim, J. Mol. Biol. 319 (2002) 421-431.

[5] W. Wang, R. Kim, Proc. Natl. Acad. Sci. 98 (2001) 8525-8530.

[6] P. F. Conzen, M. Nuscheler, A. Melotte, M. Verhaegen, T. Leupolt, H. V. Aken, K. Peter, Anesthesia & Analgesia 81 (1995) 569-575.

[7] V. L. Richmond, A. J. Clin Nutr. 41 (1985) 129-138.

[8] O.E. Eissaa, E: M. El-Shourbagy, S. A. Ghobashy, Tanta Dental Journal 10 (2013) 86-96.

[9] E. T. Everett, J. Dent. Res. 90 (2011) 552–560.

[10] M. Mousny, S. Omelon, L. Wise, E. T. Everett, M. Dumitriu, D. P. Holmyard, X, Banse, J. P. Devogelaer, M. D Grynpas, Bone 43 (2008) 1067–1074.

[11] H. Bouaziz, L. Soussia, F. Guermazi, N. Z. Sfax, Tunisia, Fluoride 38 (2005) 185–192.

[12] Y. Wang, R. Song, K. Guo, Q. Meng, R. Zhang, X. Kong , Z. Zhang, Dalton Trans. (2016)

[13] Z.-h. Lin, Y.-g. Zhao, C.-y. Duan, B.-g. Zhang, Z.-p. Bai Dalton Trans. (2006) 3678–3684.

[14] Z.-h. Lin, S.-j.Ou, C.-y. Duan, B.-g. Zhang, Z.-p. Bai, Chem. Commun., (2006) 624–626.

[15] A. Mohammadi, J. Jabbari, Can Chem, 94 (2016) 631-636

[16] P. Ghosh, N. Kumar, S. K. Mukhopadhyay, P. Banerjee, Sensor Actuat. B-Chem 224 (2016) 899–906.

[17] Parvej Alam, Vishal Kachwal, Inamur Rahaman Laskar Sensor Actuat. B-Chem 228 (2016) 539–550.

[18] Yan-Li Leng a,b, Jian-Hui Zhang b, Qiao Li a, You-Ming Zhang a, Qi Lina, Hong Yao a, Tai-Bao Wei, Spectrochim. acta A 167 (2016) 116–121.

[19] M. S. Frant, J. W. Ross, Science 154 (1966) 1553–1555.

[20] G. Xu, M. A. Tarr, *Chem. Commun.* (2004) 1050-1051.

[21] Y. M. Hijji, B. Barare, A. P. Kennedy, R. Butcher, Sensor Actuat. B-Chem. 136 (2009) 297–302.

[22] S. Dalapati, S. Jana, N. Guchhait, Spectrochim. acta A 129 (2014) 499–508.

[23] S. Dalapati, M. A. Alam, S. Jana, S. Karmakar, N. Guchhait, Spectrochim. acta A 102 (2013) 314–318.

[24] R. Acher, Proteins and Nucleic Acids, Comprehensive Biochemistry, Elsevier Publishing Company, New York, 1963, vol. 8.

[25] S. Das, G. S. Kumar, J. Mol. Struct. 872 (2008) 56–63.

[26] I. Saha, M. Hossain, G. S. Kumar, J. Phys. Chem. B, 114 (2010) 15278–15287.

[27] R. Palchaudhuri, P. J Hergenrother, Curr. Opin. Biotechnol. 18 (2007) 497–503.

[28] A. M. Tomuta, X. Ramis, F. Ferrando, A. Serra, Progress in Organic Coatings. 74 (2012) 59-66.

[29] Z. Lin, Y. Zhao, C. Duan, B. Zhang, Z. Bai, Dalton Trans. (2006) 3678–3684.

[30] L. S. Evans, P. A. Gale, M. E. Light, R. Quesada, Chem. Commun. (2006) 965–967.

[31] M. Boiocchi, L. D. Boca, D. E. Gomez, L. Fabbrizzi, M. Licchelli, E. Monzani, J. Am. Chem. Soc. 126 (2004) 16507–16514.

[32] Y. M. Hijji, B. Barare, A.P. Kennedy, R. Butcher, Sensor Actuat B-Chem. 136 (2009) 297–302.

[33] J. Yoo, M. -S. Kim, S. -J. Hong, J. L. Sessler, C. -H. Lee, J. Org. Chem. 74 (2009) 1065–1069.

[34] K. S. Moon, N. Singh, G. W. Lee, D. O. Jang, Tetrahedron. 63 (2007) 9106–9111.

[35] H. A. Benesi, J. H. Hildebrand, J. Am. Chem. Soc. 71 (1949) 2703–2707.

[36] I. D. Kuntz, F. P. Gasparro, M. D. Johnston, R. P. Taylor, J. Am. Chem. Soc. 90 (1968) 4778–4781.

[37] (a) G. L. Long and J. D. Winefordner, Anal. Chem. 55 (1983) 712A-724A, (b) A. Bhattacharyya, S. Ghosh and N. Guchhait, RSC Adv. 6 (2016) 28194-28199.

[38] J. J. Park, Y.-H. Kim, C. Kim, J. Kang, Tetrahedron Lett. 52 (2011) 3361–3366.

[39] X. P. Bao, J. H. Yu, Y. H. Zhou, Sensor Actuat B-Chem. 140 (2009) 467–472.

[40] S. Dalapati, M. A.Alam, S. Jana, N. Guchhait, J. Fluorine Chem.132 (2011) 536-540.

[41]M. M. Islam, M. Chakraborty, P. Pandya, A. A. Masum, N. Gupta, S. Mukhopadhyay, Dyes Pigm. 99 (2013) 412-422.

[42] A. A. Masum, M. Chakraborty, P. Pandya, U.C. Halder, M. M. Islam, S. Mukhopadhyay, J. Phys. Chem. B. 118 (2014) 13151–13161.

[43] P.D. Ross, S. Subramanian, Biochem. 20 (1981) 3096–3102.

[44] G. Zhang, P. Fu, L. Wang, M. Hu, J. Agric. Food Chem. 59 (2011) 8944–8952.

Figure captions

Fig.1. Naked-eye color changes of compound **1** (1.0×10^{-4} M) after addition of 2 equivalent of various anions in aqueous dimethyl sulphoxide solvent (DMSO:H_2O =7:3, v/v).

Fig. 2. UV-Vis spectral changes of compound **1** (1.0×10^{-6} M) upon addition of F^- ion (0–5 equiv.) in aqueous dimethyl sulphoxide solvent (DMSO:H_2O =7:3, v/v)..

Fig. 3. ^{1}H NMR spectra of compound **1** in DMSO-d_6 after addition of 0-5 equivalent of fluoride ion.

Fig. 4. Color change of test paper containing **1** (10^{-4} M) in presence of different anions.

Fig. 5. Ground state optimized structure of compound **1.**

Fig. 6. a) Circular dichroic spectral profile of DNA in different ratio of DMSO and water **(v/v)** Inset: change of ellipticity *vs* concentration of DMSO b) Circular dichroic spectral profile of DNA (40 mM) with increasing compound **1** concentration.

Fig. 7. Absorption of compound **1** in the presence of increasing concentration of DNA (Scatchard analysis inset).

Fig. 8. Van't Hoff plot for the binding of 1 with CT-DNA.

Fig. 9. Thermal melting profiles of DNA and the **1**–DNA complex as constructed by observing the relative absorbance at λ_{abs} = 260 nm as a function of temperature.

Fig. 10. Molecular docking using MOE. (a) Docking picture of **1** to the minor groove of DNA, (b) Hydrogen bonds between compound **1** and DNA bases (indicated with the distances), (c) Two-dimensional interaction diagram of compound **1**−DNA system (buttons with A and T represent adenine and thymine bases in DNA.

Table 1. Some useful Some useful bond lengths (Å)of compound 3 and 3. F– complex of compound **1** and **1**. F^- complex

Substrates	**H1…O1**	**H1–O3**	**H2…O2**	**H2–O4**	**N-H3...F$^-$**	**N-H4...F$^-$**	**C-H5...F$^-$**
1	2.108	2.277	2.108	2.277	---	---	---
1 + F^-	2.066	2.260	2.575	2.144	2.220	1.692	2.106

Table 2. List of four DNA Decamer Sequences used for Docking Study

S.No.	**DNA**	**Sequence**
1	S1	5'-d(GATGGCCATC)$_2$
2	S2	5'-d(GATCCGGATC)$_2$
3	S3	5'-d(GGCAATTGCC)$_2$
4	S4	5'-d(GGCTTAAGCC)$_2$

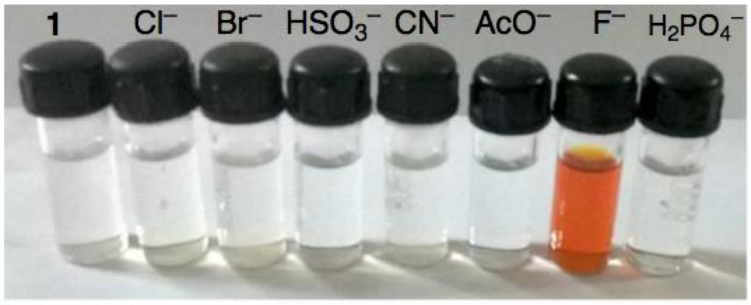

Fig. 1

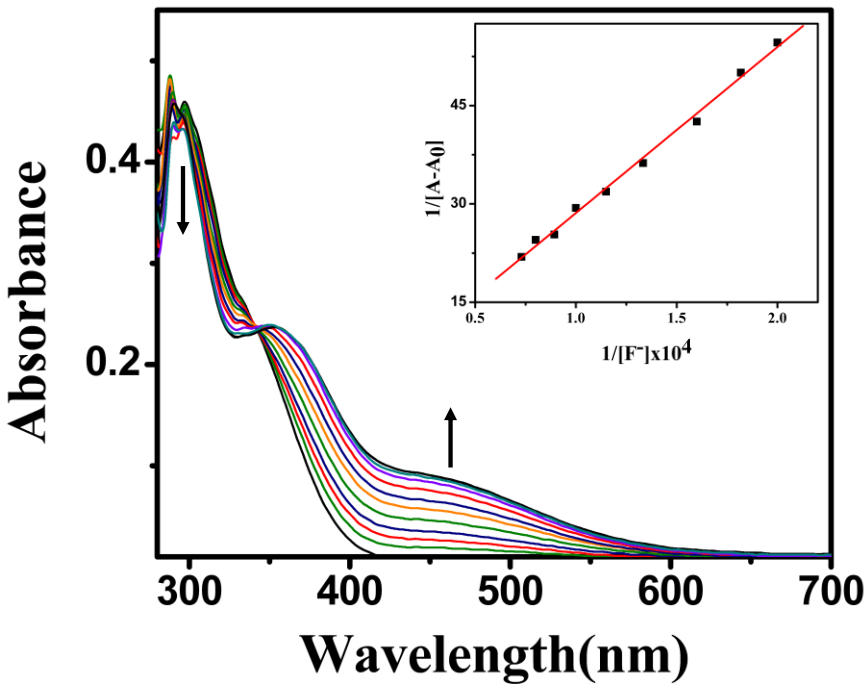

Fig. 2

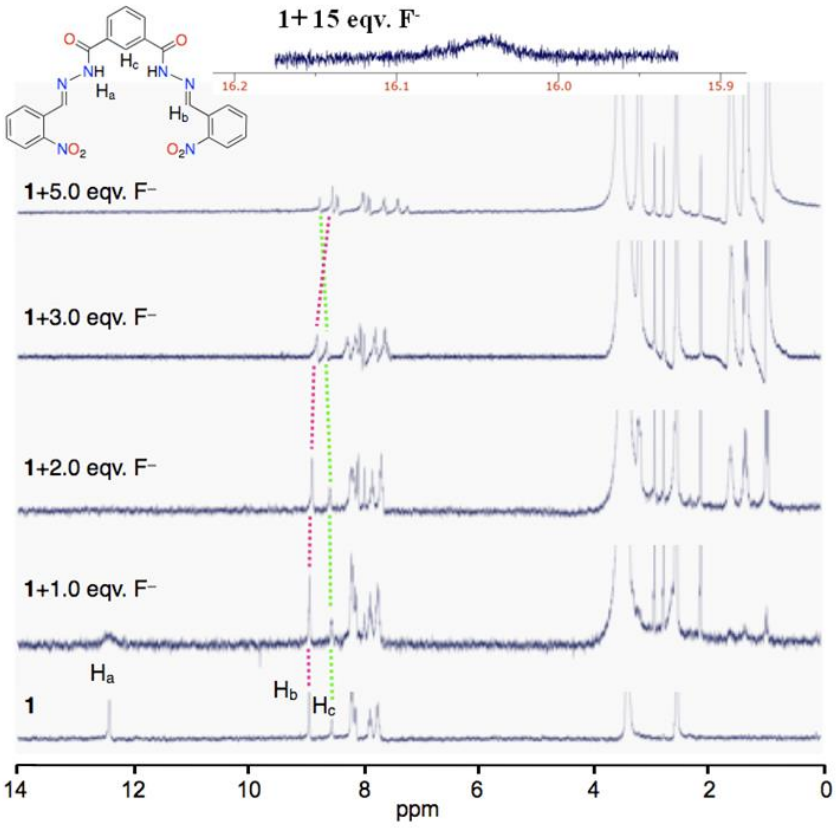

Fig. 3

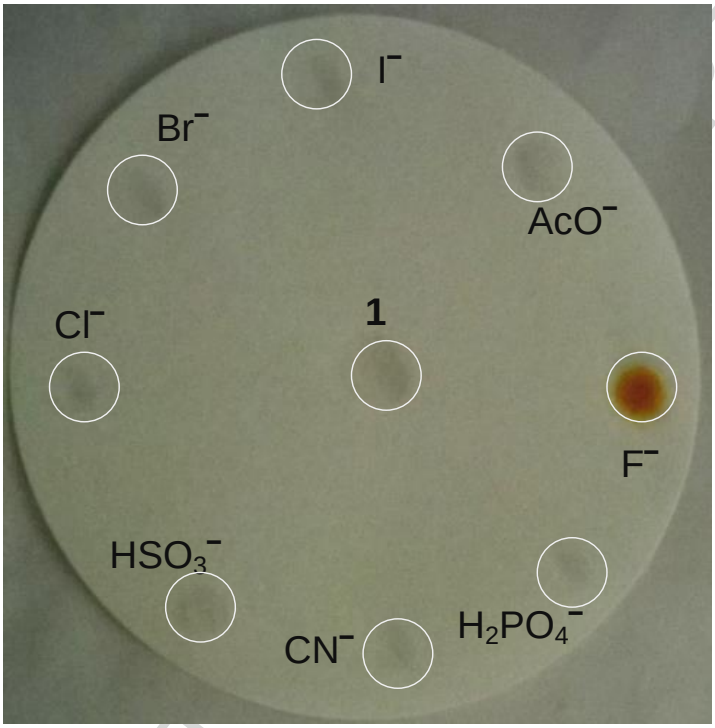

Fig. 4

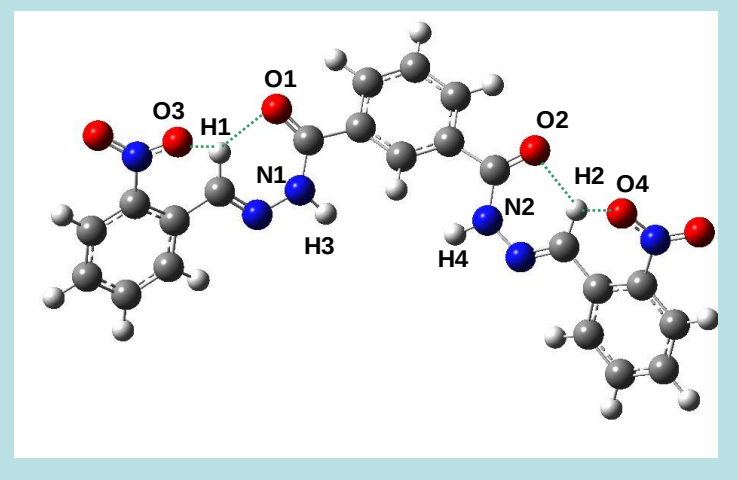

Fig. 5

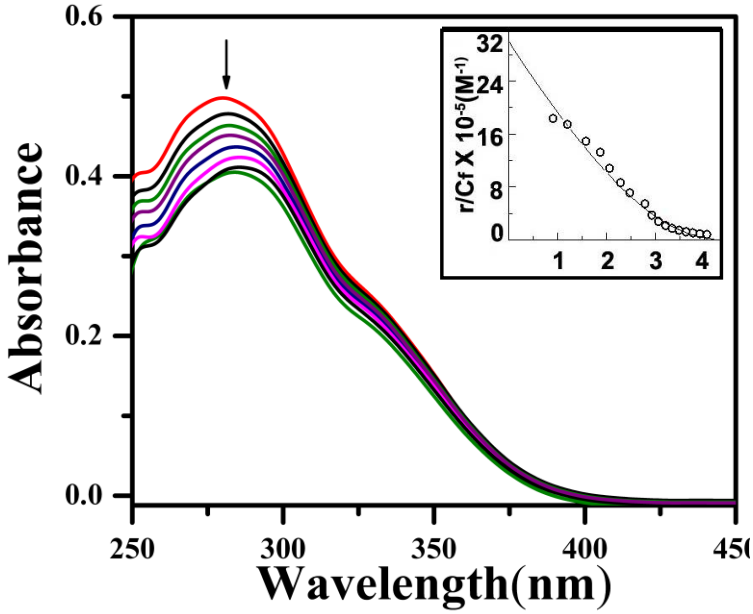

Fig. 6

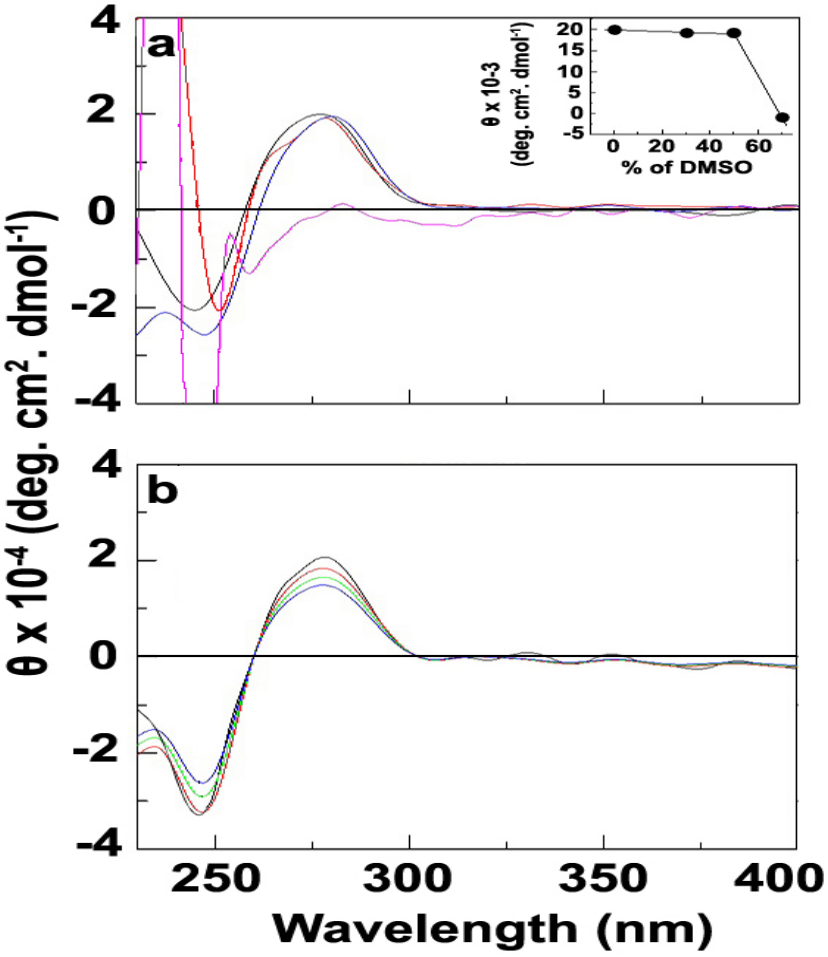

Fig. 7

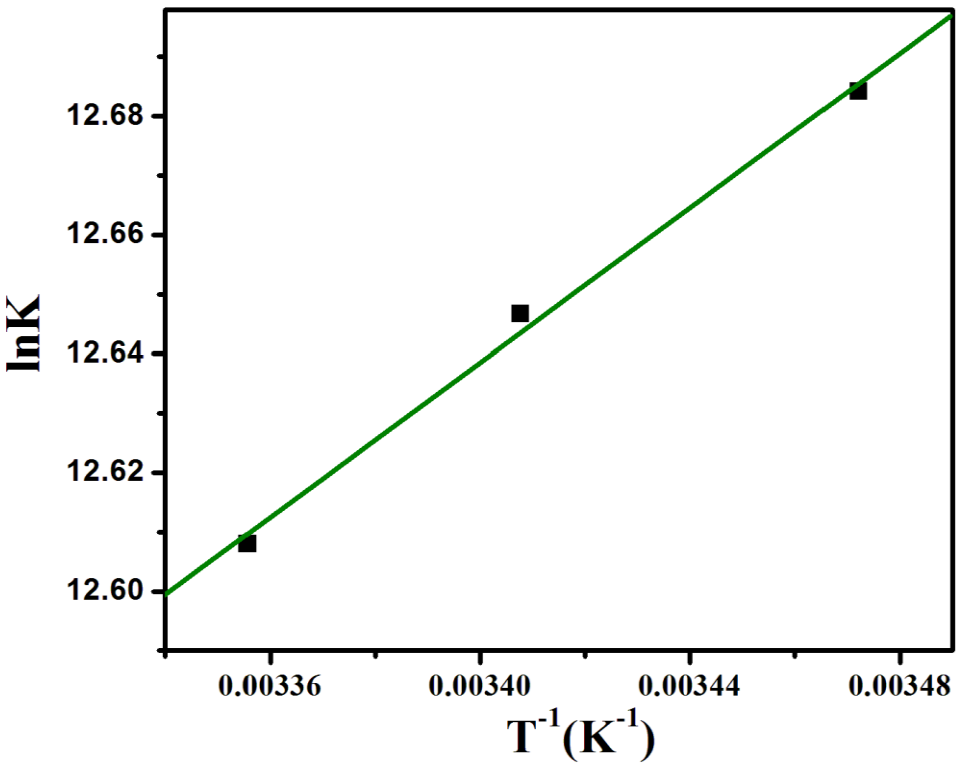

Fig. 8

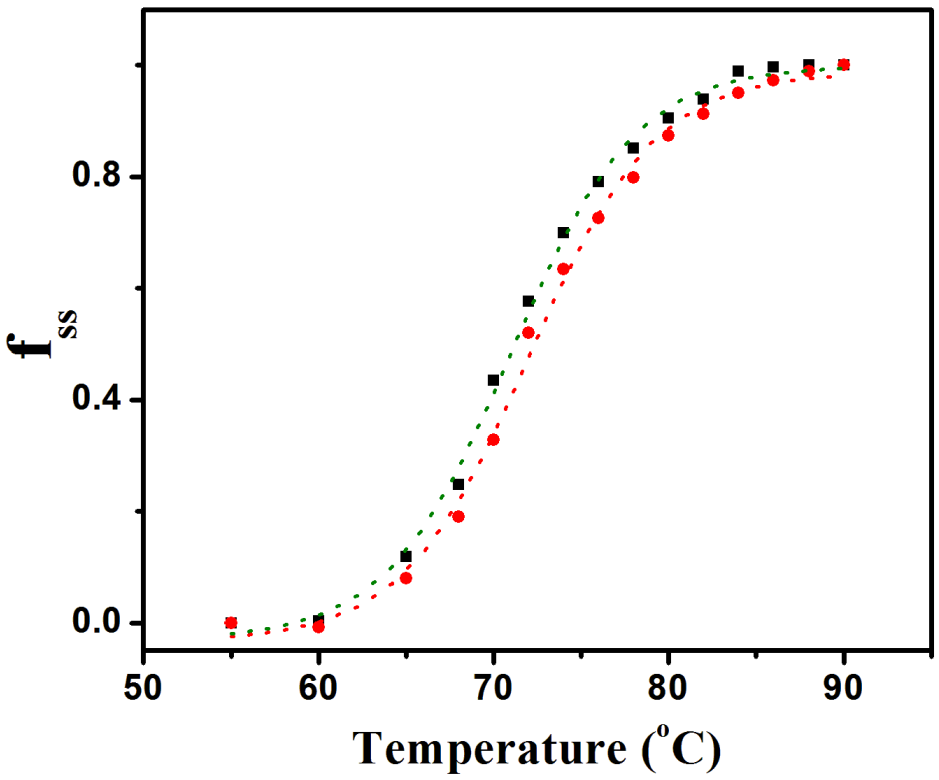

Fig. 9

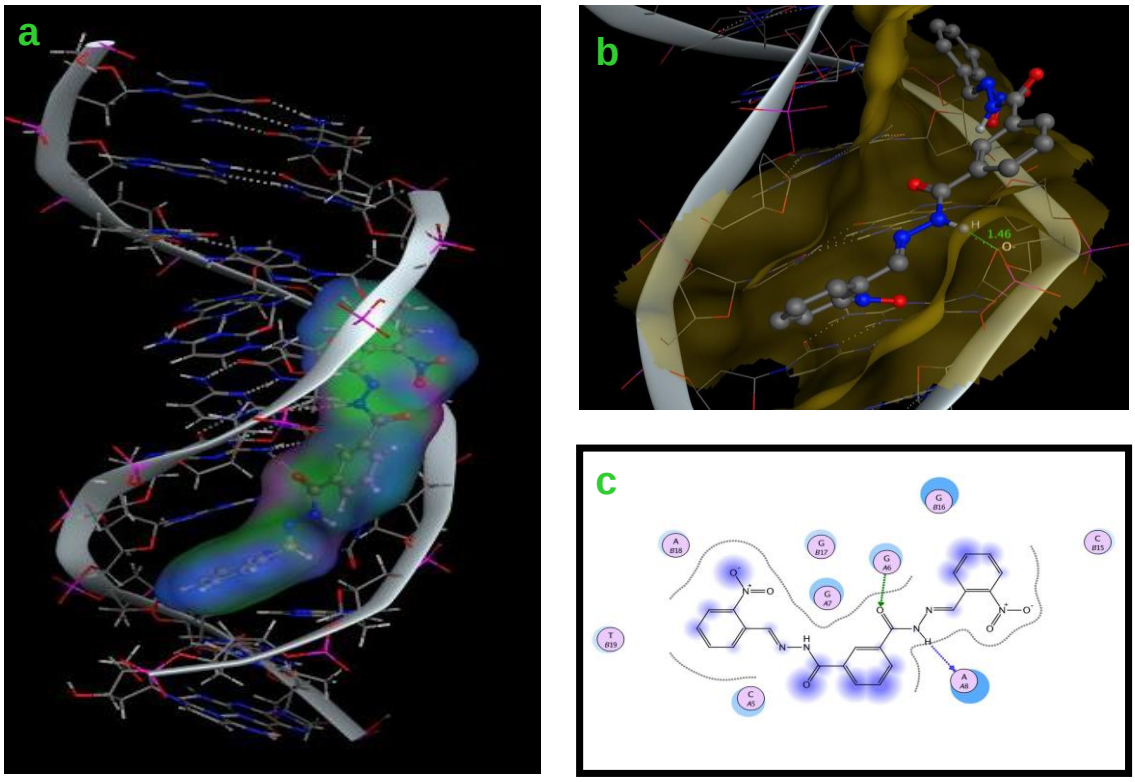

Fig. 10

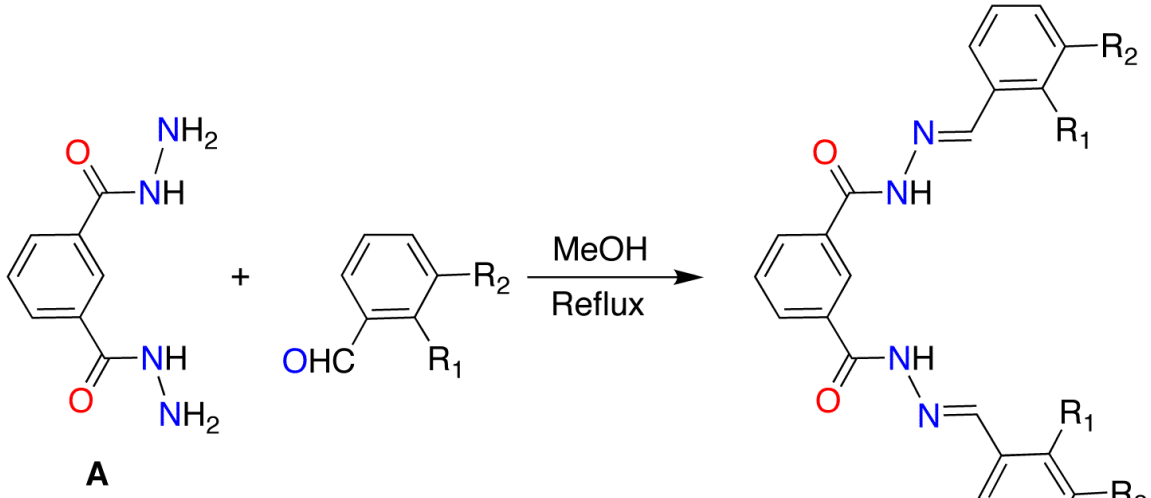

Receptors	R_1	R_2
1	$-NO_2$	–H
2	–H	$-NO_2$
3	–H	–H

Scheme I. Syntheses of receptors **1**, **2**, and **3**

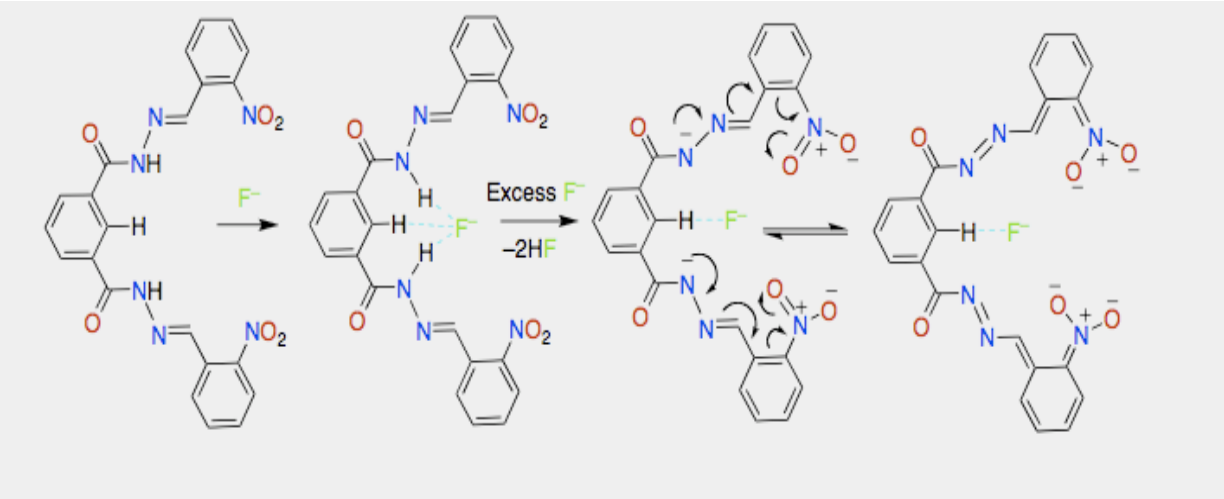

Scheme II. The plausible resonance representation of the deprotonated form of receptor **1**

Graphical abstract

A selective chemosensor for fluoride ion and its interaction with Calf Thymus DNA

Soumen Ghosh[a], Abdulla Al Masum[b], Aniruddha Ganguly[a], Md. Maidul Islam[b], Md. Akhtarul Alam[b]* and Nikhil Guchhait[a]*

[a]*Department of Chemistry, University of Calcutta, 92 A. P. C. Road, Calcutta-700009, India*

[b]*Department of Chemistry, Aliah University, IIA/27, New Town, Kolkata-700 156, West Bengal, India*

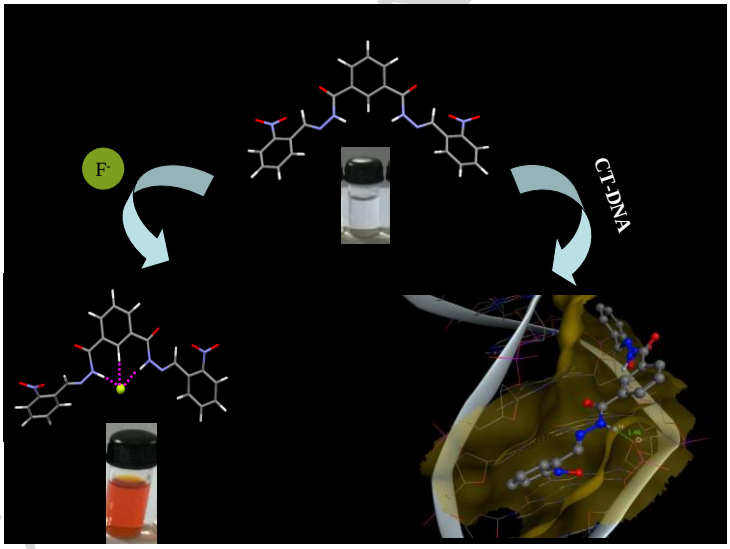

Research highlights

► A new synthetic amido-Schiff base for selective detection of Fluoride ion in semi-aqueous medium.

► Color change of the sensor in presence of F^- has been detected by naked-eye.

►Test paper coated with this amido-schiff bases can be used as test kit.

► The colour change of the compound is influenced by position of nitro group.

► Compound **1** can effectively interact with CT-DNA which has been studied by both spectroscopically and Molecular docking.